High Resolution Radar Imaging of Urban Areas

UWE STILLA, München

ABSTRACT

New synthetic aperture radar (SAR) sensors on satellites like TerrsSAR-X allow flexible mapping with a large coverage or a high resolution of about one meter. Leading-edge airborne SAR sensors provide spatial resolutions on the order of a decimetre. In such data, many features of urban objects can be identified, which were beyond the scope of radar remote sensing before. But, SAR images are often really difficult to be interpreted: the presence of speckle as well as of some distortion effects, like shadowing and layover, makes the analysis of this kind of image complex. The impact of high resolution SAR data on the analysis of urban scenes and typical SAR effects are discussed. Examples for the appearance of buildings and other man-made objects are given..The benefit of SAR-simulation is addressed and examples are shown. Finally, typical problems in SAR smulation is discussed.

1. INTRODUCTION

Nowadays, in every country urban areas are growing and expanding. Information about urban structures and their temporal changes is very important for monitoring health conditions of urban centers and planning purposes in different fields. Depending on the task the requirements concerning, resolution, precision, coverage, reliability, repetition, actuality, reliability, etc. are very different and are crucial for the optimal platform (e.g. airborne or spaceborne) and sensor system (e.g. optical, infrared, lidar, or radar).

In increasing demand on high resolution sensors systems can be observed for analyzing urban areas and man-made objects. Due to the poor spatial resolutions of provided images in the passed decades, an Earth mapping by satellite imagery has been mainly limited to natural landscapes. Often the phenomena to be observed did not need high image resolution as they could be monitored on scales of many tens of meters. But, this is not sufficient for urban areas. Here, the main structure of the objects in the scene (buildings, streets, etc..) has dimensions that are often in the scale of tens of meters while many other items are even smaller (windows, balconies, cars and so on). Consequently, high resolution is an important requirement for an adequate, not coarse description of this kind of scene.

Fig. 1: Section of the first TerraSAR-X image (19 June 2007) South Russian Steppes (about 50 kilometres west of Volgograd), DLR, Astrium

Fortunately, in the last decades new technologies have been developed to this aim. In the field of remote sensing, an important role is played by satellite systems with high resolution sensors working in optical and radar domain. In the optical domain IKONOS and QUICKBIRD capture images with a ground sampling distance (GSD) of 1 m and better.

Figure 2 shows a section of test area TUM in Munich, Germany, taken by IKONOS. For comparison an aerial image of the same area with a GSD of 10cm is shown in Fig. 4.

Fig. 2: Satellite image of Munich, Test area TUM, GSD: approx. 1m x 1m, IKONOS

Fig. 3: SAR image of Munich, Test area TUM, Resolution: 2.0 m x 3.0 m (Range x Azimuth), GSD: approx. 0.7m x 0.7 m, E-SAR, DLR-HR

In contrast to optical sensors Synthetic Aperture Radars (SAR) allow working day and night and in almost all weather conditions. Upcoming satellite systems will achieve significant improvement of geometric resolution that is expected to be in the order of few meters. Figure 3 shows a SAR image of the E-SAR system which serves as an example for this resolution. The German radar satellite TerraSAR-X was launched on 15 June 2007 and is able to operate in the "Spotlight" mode with 10 x 10 km scenes at a resolution of 1-2 meters. Larger scenes can be captured with a lower resolution (3-6 m) in the "Stripmap" mode with 30 km wide strips or in the "ScanSAR" mode (16 m) with 100 km wide strips. A section of the first image captured in Stripmap mode is shown in Fig. 1. Independent of the TerraSAR-X mission first satellites with very high resolution sensors were successfully launched within the German defense program “SAR Lupe”. Modern airborne SAR systems provide spatial sampling with decimeter spacing. An example of an SAR image taken by the MEMPHIS sensor is shown in Fig. 5.

Fig. 4: Aerial image of Munich, Test area TUM,, GSD: approx. 0.1 m x 0.1 m, AEROWEST/GOOGLE INC.

Fig. 5: SAR image of Munich, Test area TUM, GSD: approx. 0.2 m x 0.2 m, MEMPHIS, FGAN-FHR

All images of Fig. 2 to Fig. 5 allow recognizing urban structures like building complexes. Whereas in optical images of high resolution building details can be intuitively extracted (Fig. 6 and Fig. 8), SAR images need knowledge about basic effects for interpretation (Fig.7 and Fig. 9).

Fig. 6: Section of Fig. 2

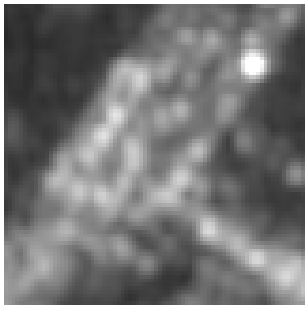

Fig. 7: Section of Fig. 3

Fig. 8: Section of Fig. 4

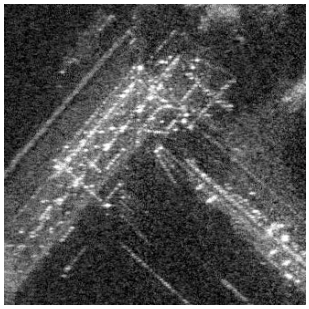

Fig. 9: Section of Fig. 5

2. MAN-MADE OBJECTS IN SAR IMAGES

2.1. Displacement by elevated objects

In contrast to electro-optical sensors or LIDAR, the SAR principle requires a side-looking illumination. Particularly in urban areas, phenomena like layover, shadow, multi-path signals, and speckle have to be considered. In Fig. 10 and Fig. 12 typical effects in SAR images in the vicinity of buildings are illustrated (Stilla et al., 2003; Stilla & Soergel, 2006). Let us assume a building with a vertical wall (A-B) and a flat roof (B-C) is captured in a side-looking manner from point F. In the slant range image I_S, the points A, B, C appear according to their distance to the sensor (Fig. 10). Hence, the point A on the corner line of the building appears as A' behind point B' and in-between B' and C'. The area B'A' is called the layover area. Layover occurs always at vertical building walls facing toward the sensor. It leads to a mixture of signal contributions from the building and the ground in the SAR image. Because object areas located at different positions have the same distance to the sensor, the backscatter is integrated to the same range cell. This signal integration leads to bright appearance of layover areas in SAR images.

The slant image shows a geometric distortion in range direction which makes object recognition and interpretation more difficult. For image interpretation, the data are usually sampled to a rectangular grid on the ground (Fig. 11). However, the order of the points B'', A'', C'' in the ground image I_G is still the same as in the slant image. Points A and B differing in height have the same coordinates in ground range r_G. If geocoding is carried out without DEM by projection on ground plane I_G this reversed point order can not be corrected.

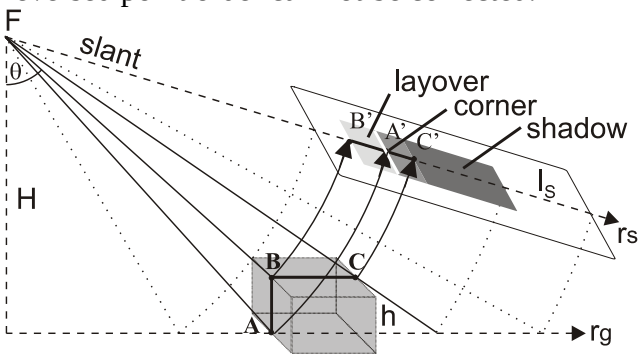

Fig. 10: Projection of a building into slant image (IS) (Stilla et al., 2003)

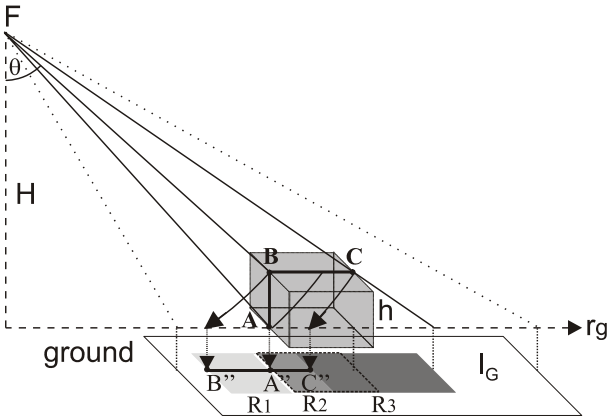

Fig. 11: Projection of a building into ground image (IG) (Stilla et al., 2003)

Perpendicular alignment of buildings to the sensor leads to strong signal responses by double-bounce scattering at the dihedral corner reflector between the ground and the building wall (Fig. 12, right). This results in a line of bright scattering in azimuth direction at the building footprint. At the opposite building side, the ground is partly occluded from the building shadow. This region appears dark in the SAR image, because no signal returns into the related range bins.

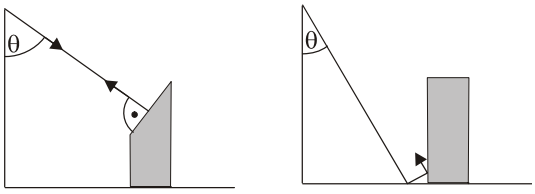

Fig. 12: Single scattering (left) and double-bounce scattering (right) at building

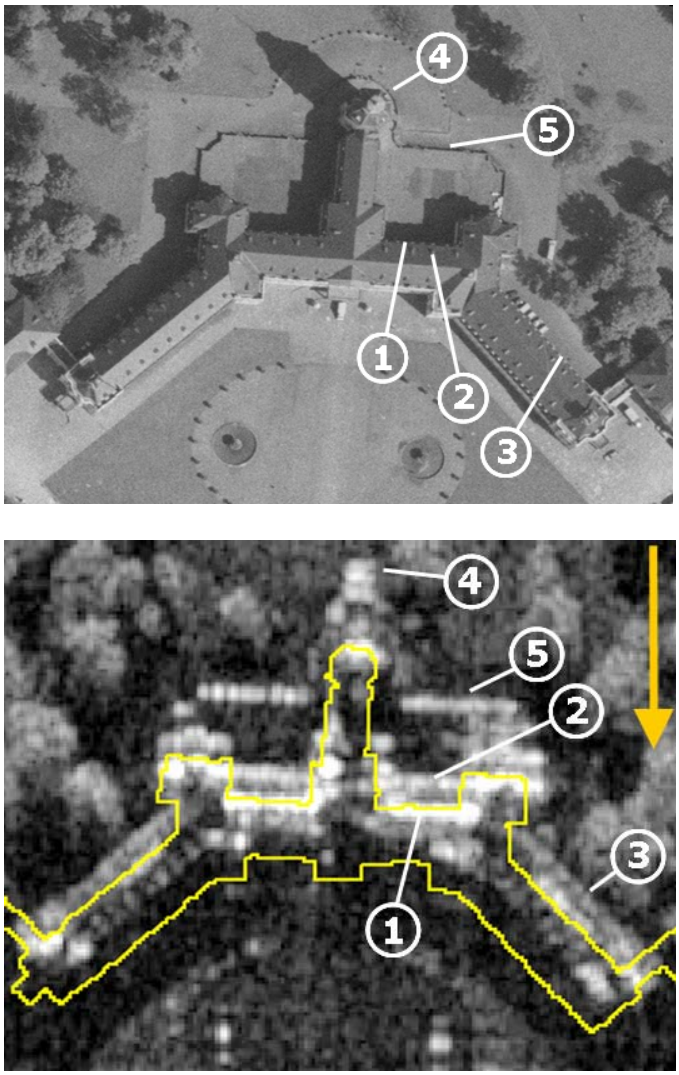

Fig. 13: Karlsruhe Castle: (top) aerial image, (bottum) SAR image overlaid with building footprints and pointers to SAR phenomena at (1) main building wall, (2) main building roof, (3) wing, (4) tower, and (5) terrace wall (SAR illumination top-down)

Besides material and roughness influence, depending on the illumination aspect the roof structure geometry may lead to strong signal response as well. The gabled building roof sketched in Fig. 12 (left) is oriented perpendicular to the sensor. Since the entire power is mirrored back to the sensor, this reflection leads to a line of dominant scattering in azimuth direction, similar to the corner reflector. This bright line caused from the roof appears closer to the sensor in the SAR image compared to the corner reflector signal. Besides the offset in range direction, both effects can be discriminated by their polarimetric properties (single-bounce respectively double-bounce).

The mentioned effects can be studied in Fig. 13 comparing the section of an aerial image and a SAR image showing the castle of Karlsruhe, Germany. The SAR image is superimposed with the building footprints from a map. The scene was illuminated from top. The signal from a corner reflector at the castle's main building is located at the building footprint (Fig. 13, Pos. 1). The bright signal from the gabled roof is projected on the terrace in front of the castle (Fig. 13, Pos 2). These two lines enclose the layover area. Layover can be observed as well at the castle wing (Fig. 13, Pos 3) and at the tower (Fig. 13, Pos 4). At the wing no line of bright scattering appears, because the double-bounce signal is reflected away from the sensor. Another double-bounce event happens at a little wall at the border of the terrace (Fig. 13, Pos 5).

The characteristic mapping of vertical objects into SAR images will be discussed using another example. Let us assume that a vertical oriented circle with diameter d is illuminated with viewing angle Θ in a way sketched in Fig. 14. The circle will be mapped into a ground image similar to the mapping of the vertical wall AB shown in Fig. 11. Point B of the circle will be mapped to point B' of the ellipse with axes a and b. The length of axis a corresponds to diameter d and the length of axis b depends on viewing angle Θ (decreasing of Θ leads to increasing of axis b of the ellipse). In case of Θ=45° we receive b=d which means that the circle is mapped to a circle in the SAR image. This is in contrast to perspective projection known from images of optical sensors where the projection results to a circle for a viewing angle Θ=90°. The mentioned effect can be seen for a Ferris wheel in Fig. 15 which was taken by a SAR image (Fig. 16) from the sketched viewing direction.

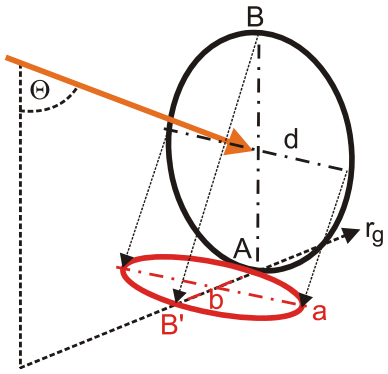

Fig. 14: Mapping of a sircle into a ground image

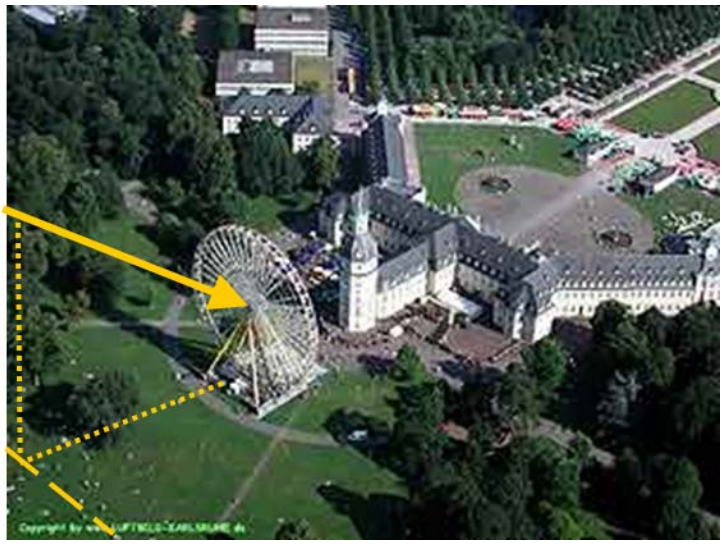

Fig. 15: Karlsruhe Castle and Ferrs wheel The arrow shows range direction (from north to south)

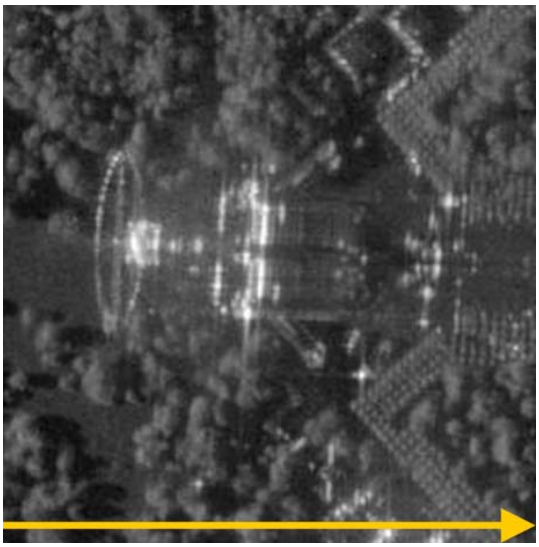

Fig. 16: SAR image (range: left to right) (see Fig. 15)

2.2. Displacement by moving objects

For processing a SAR image from a single aperture all scene objects will be assumed stationary. The relative motion between sensor and scene causes a Doppler frequency shift, which is exploited to achieve a high azimuth resolution and to determine the correct azimuthal position of objects. The movement of objects causes artifacts. The radial velocity component of the movement leads to an azimuthal displacement (because of the additional Doppler frequency shift), the parallel component leads to blurring. These effects are exploited by different approaches to detect moving objects and to determine object's velocity (see e.g. Hinz et al, 2006). The azimuthal displacement of a moving object is illustrated in Fig .17.

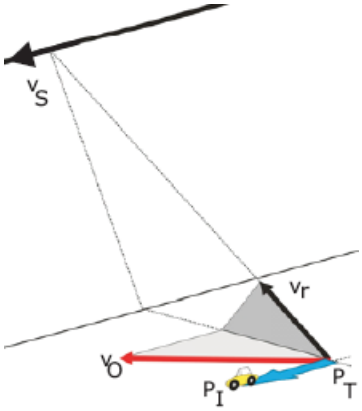

Fig. 17: Azimuthal displacement of a moving object

Let v_S the direction of the moving sensor and v_O the vector of object velocity, then v_r represents the component of v_O in range direction. In the situation depicted in Fig. 17 v_r points towards to the sensor (opposite range direction) which results in a displacement of the object in flight direction from its true position P_T to the position P_I. In case that v_r points in range direction (away from the sensor) the displacements vector points to the anti parallel direction of the flight path. The effect caused by a moving object can be found in the first TerraSAR-X image (Fig. 1), too. A bright line can be recognized in Fig. 18 (bottom, right) which seems to be displaced from the track and caused by a moving train.

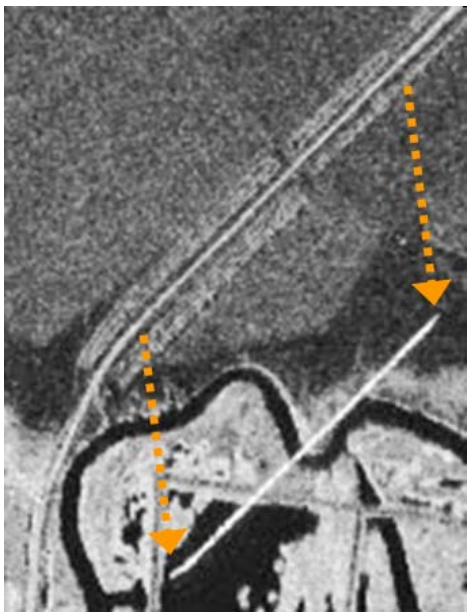

Fig. 18: Moving train (Section of Fig. 1), v ≈ 40 km/h, dispacement ≈ 800 m

2.3. Displacement by elevated and moving objects

Let us come back to the scene shown in Fig. 15. During a second flight the same scene was captured by a flight path (south to north) perpendicular to the first flight path (east to west) (see arrow in Fig. 19). One would expect according to Fig. 21 that point B is shifted towards the sensor and that the circle appears like a line due to the side-looking view towards the circle. However, Fig. 20 shows a different appearance of the Ferris wheel than expected. In the image an ellipse is visible with a main axis oriented perpendicular to the circle. How can this explained?

Let us assume the Ferris wheel has rotated during the acquisition of the SAR data (Fig. 22). In this case tangential velocity vectors can be assigned to each gondola of the Ferris wheel. These vectors point more or less towards or opposite to the sensor. According to the component of the velocity vector in this direction, a displacement occurs with a corresponding magnitude (Fig. 23). The mapping of all scatter (gondola) forms an ellipse in the ground range image (Fig. 24). This effect can be observed in Fig. 20. The size of the axis perpendicular to ground range changes with the rotation velocity (see Fig. 20 and Fig. 25).

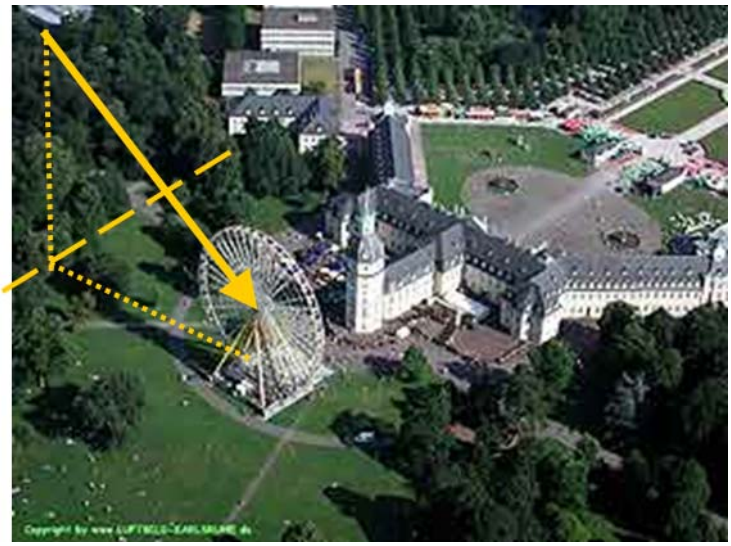

Fig. 19: Karlsruhe Castle and Ferrs wheel. The arrow shows range direction (from east to west)

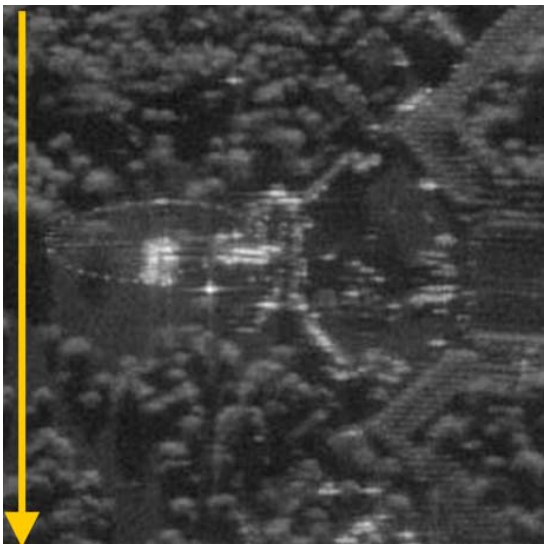

Fig. 20: SAR image (range: top - down) (see Fig. 19)

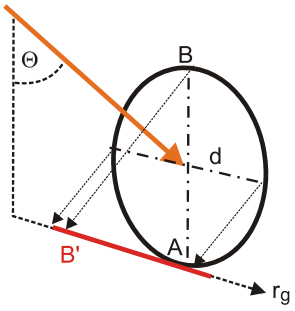

Fig. 21: Expected appearance

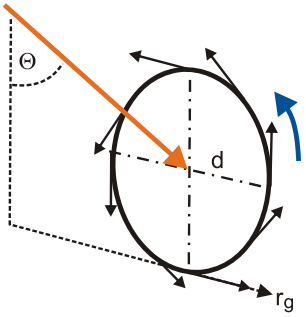

Fig. 22: Velocity vectors of moving points

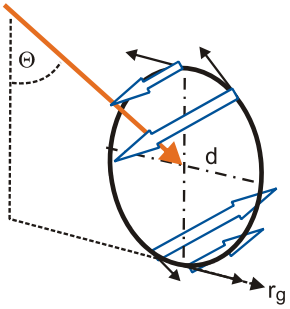

Fig. 23: Displacement vectors of some points

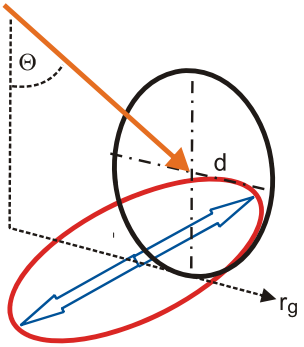

Fig. 24: Mapping of moving points on ground range

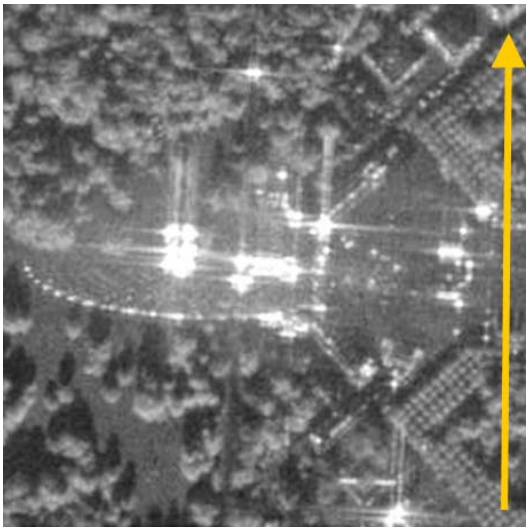

Fig. 25: SAR image (range: bottum - up)

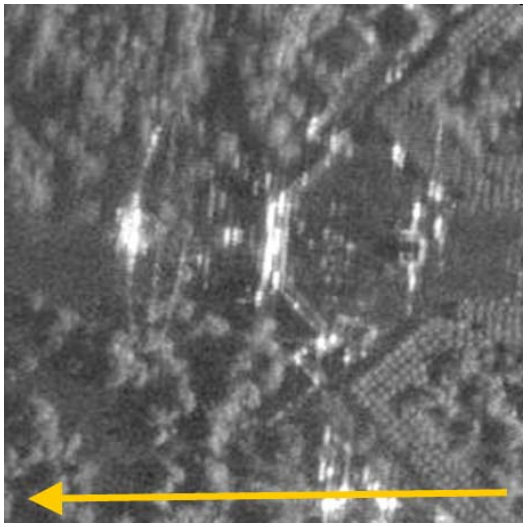

Fig. 26: SAR image (range: right to left)

3. SIMULATION OF SAR IMAGES

The mentioned effects show that interpretation of scene details can be a difficult in scenes with many man-made structures, e.g. given in urban areas like city centers or industrial areas. From a given model of the scene and a model of the sensor the expected complex radar signal or a SAR image can be computed by a simulation. Simulators can be divided into a group generating the raw signals which has to be further processed for receiving an image and a group outputting just an image.

Concerning the first group some simulators are designed to investigate different sensor configurations, others are designed to generate images as realistic as possible considering electromagnetic properties of the object surfaces. Often the received scene information is divided into cells according to the resolution in range and azimuth and a Point Scattering Model is used to calculate the backscattering from each cell. Considering a speckling distribution an image is assembled from this input data. Special attention has to be paid to reflections between object surfaces which may result in strong reflections at corners and typical geometric effects visible in real SAR images. The simulation of double and multiple bounce effects requires considerable computational effort. Different to the usage of cells and a point scattering model, planes can be derived from a digital elevation model and the local incidence angles are considered to calculate the

backscattering. Figure 27 shows an example for the simulation of an SAR image using this technique (Franceschetti et al., 2007). The scene model was derived from laser elevation data of the test area TUM. Generally, the computational effort of the mentioned approaches for broader scenes is high and the simulation is time consuming which makes is unsuitable for real time applications, e.g. to vary interactively model parameters.

For overcoming this draw back the second group of approaches relinquishes the claim to generate SAR raw data and outputs an image. One idea is to do without a perfect simulation by considering interaction of objects and to simulate single objects of the scene separately. The final SAR image is assembled with results of single objects and a background.

In contrast to a simulation of the intensities for some investigations just a visualization of certain SAR effects is required. Let us take, for example, the question about the shadow area in total given by a city model and a radar illumination by given angles or the question about areas not affected by a certain SAR effect. For answering this questions maps showing areas of shadow, layover, or a combination of both are helpful and sufficient (Stilla et al., 2003, Soergel et al., 2003). This allows (e.g. for traffic monitoring applications) to determine the percentage of road area which will be visible assuming given parameters of a planned flight campaign (Stilla et al., 2004).

Similar to the visualization of SAR effects mentioned before SARViz (Balz, 2007) allows a fast visualization exploiting the capability of graphic processing units (GPU). For this task the geometry of SAR images is considered in the vertex stage and the radiometry is considered in the pixel shader of the graphic board. Fig. 28 shows an example for the visualization by SARViz using the same laser elevation data as used in Fig. 27.

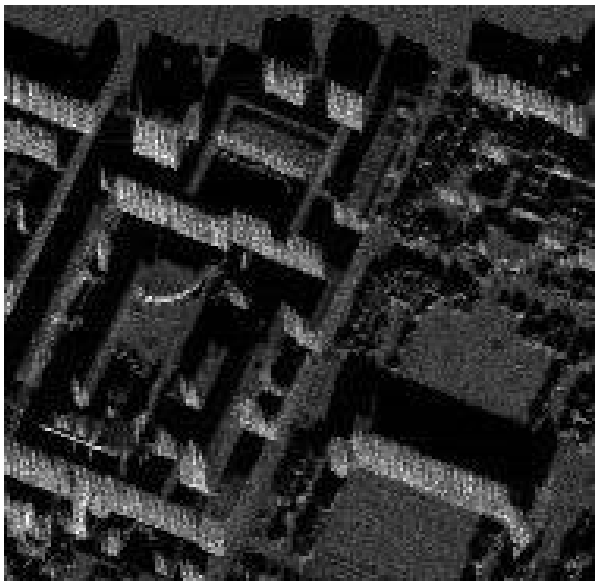

Fig. 27: SAR raw signal simulation (Franceschetti et al., 2007) (direction of range: from bottom to top)

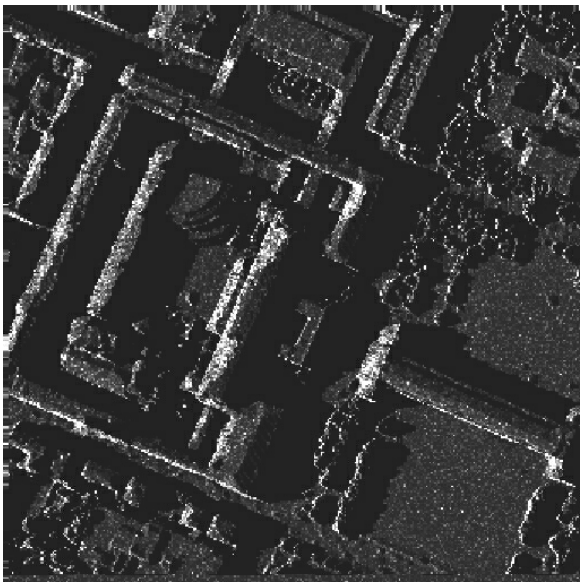

Fig. 28: Visualization of SAR effects using SARViz (Balz, 2007)(direction of range: from left to right)

4. DISCUSSION

With increasing resolution of SAR images a consideration of geometric effects becomes more and more important (Stilla et al., 2005). Simulation of SAR images may be very helpful for visualization the mentioned effects and understanding the scene. However, a problem in simulation of SAR data or SAR images with high resolution is the lack of adequate scene data. In case of simulating raw data the electromagnetic properties of surfaces (e.g. facades, roofs, roads etc.) are required. Supposing the geometry of a city area will be available by building models, how should surface materials be determined and their moisture be estimated? This additional information has to be captured by time consuming field work. The second problem is that available building models generally do not contain sufficient details for calculating the dominating effects in SAR images of urban areas. A chimney, a gutter, antennas, or small structures on the roof illuminated by the radar beam from a certain direction may result in a high backscattering whereas the roof itself may scatter the radiation not in direction of the sensor and stay invisible. Nevertheless, humans often do not

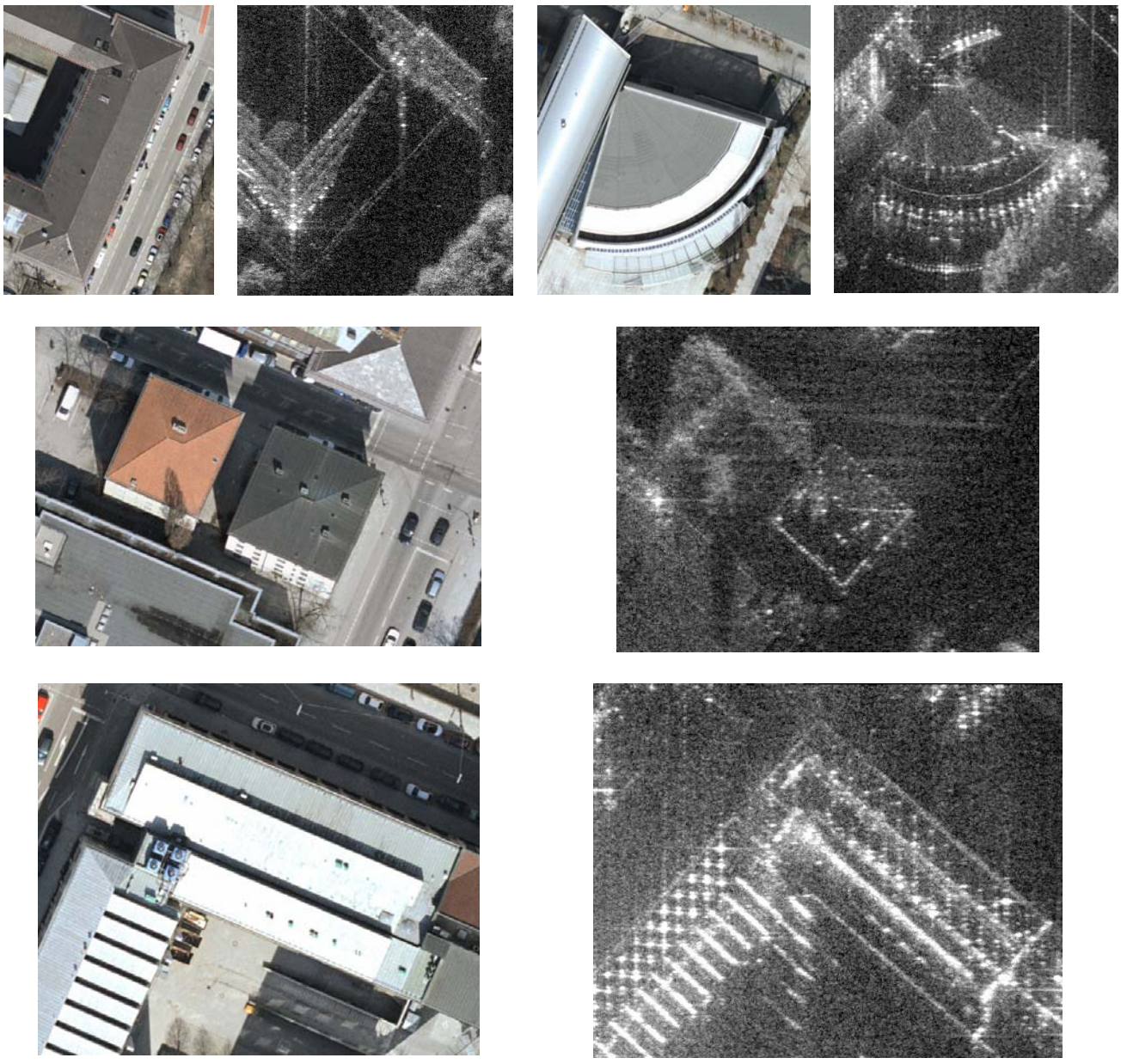

Fig. 29: Comparison of sections from Fig.4 and Fig. 5

have any problem in recognizing a building or a roof by some details or few contours, e.g. ridge and gutters (see Fig. 29). For receiving the same appearance minor details have to be captured in building models and to be simulated.

5. ACKNOWLEDEGEMENTS

The author would like to thank Prof. Ender, Dr. Essen and Mr. Brehm at Research Institute for High Frequency Physics and Radar Techniques (FHR), Forschungsgesellschaft für Angewandte Naturwissenschaften e.V. (FGAN) for supplying the MEPHIS data of Karlsruhe and Munich. He is also grateful to the Microwaves and Radar Institute, German Aerospace Center (DLR) for providing the E-SAR data of Munich.

6. REFERENCES

Balz, T. (2007) Echtzeitvisualisierung von SAR-Effekten mittels programmierbarer Grafikhardware. PhD Thesis. University of Stuttgart

Franceschetti, G., Guida, R., Iodice, A., Riccio, D., Ruello, G., Stilla, U. (2007) Simulation tools for interpretation of high resolution SAR images of urban areas. 2007 Urban Remote Sensing Joint event: URBAN2007-URS2007

Hinz, S., Bamler, R., Stilla, U. (2006) Theme Issue: Airborne und Spaceborne Traffic Monitoring (eds) ISPRS Journal of Photogrammetry and Remote Sensing, 61

Soergel, U., Schulz, K., Thoennessen, U., Stilla, U. (2003): Event-drivenSAR data acquisition in urban areas using GIS. GeoBIT/GIS, J. Spat. Inf. Decis. Mak., 2003, 12, pp. 32–37

Stilla, U., Soergel, U., Thoennessen, U. (2003): Potential and limits of InSAR data for building reconstruction in built-up areas, Journal of Photogrammetry and Remote Sensing, 58(1–2), pp. 113–123

Stilla, U., Michaelsen, E., Soergel, U., Hinz, S., Ender, H. J. (2004): Airborne monitoring of vehicle activity in urban areas. In: Altan MO (ed) International Archives of Photogrammetry and Remote Sensing. Vol 35, Part B3, pp. 973-979

Stilla, U., Soergel, U., Thoennessen, U., Brenner, A. (2005) Potential and limits for reconstruction of buildings from high resolution SAR data of urban areas. Proceedings of 28th General Assembly of International Union Radio Science (URSI), New Delhi, (on CD)

Stilla, U., Soergel, U. (2006): Reconstruction of buildings in SAR imagery of urban areas. In: Weng, Q., Quattrochi, D.A. (eds) Urban Remote Sensing. Boca Raton, FL: Taylor & Francis, pp. 47-67